Prediction of the Glass Transition Temperature of Multicyclic and Bulky Substituted Acrylate and Methacrylate Polymers Using the Energy, Volume, Mass (EVM) QSPR Model

Christopher C. Cypcar,† Philippe Camelio, Veronique Lazzeri,* Lon J. Mathias,*,† and Bernard Waegell

Laboratoire d'Activation Sélective en Chimie URA CNRS 1409, Faculté des Sciences et Techniques St. Jérôme, Avenue Escadrille Normandie-Nièmen - Case 532, 13397 Marseille, France

Received August 5, 1996; Revised Manuscript Received October 16, 1996[⊗]

ABSTRACT: Described here is a QSPR equation for calculating glass transition temperatures for acrylate and methacrylate polymers, especially those with bulky ester substituents. This approach is based on molecular mechanics calculations and exclusively involves a force field to describe a particular polymer system; i.e., no group additivity values are required. Results from two different force fields yielded similar results, indicating that this model is not dependent on a particular force field parameter set but rather on the atomic properties that the force field describes. The molecular mechanics calculation results (energy term), the repeat unit mass, and a measure of the volume surrounding the polymer segment (TSSV) were used to determine an energy density function that is related to experimental T_g values. This energy density function is important because it illustrates that the glass transition temperature of an amorphous polymer is related not only to the volume surrounding the polymer segment but also to its conformational energy. Limitations of other QSPR approaches (stemming from not having a particular group or bond connectivity described within the given model) are not present in this approach.

Introduction

Our recent interest in the incorporation of polycyclic and bulky substituents onto polymer backbones[1−4] has led to the need for a method to estimate the effects on properties that result from these substituents (Figure 1). These substituents have primarily been studied as glass transition temperature (T_g) modifiers.[5−11] T_g is known to increase with substituent size for rigid substituents, probably due to the increased barrier to rotation about the backbone bonds. Bulky and inflexible substituents lead to steric constraints that couple appreciably with the backbone to increase the dynamics constraints imposed on local segmental motion. It is also known that positioning the center of mass of the substituent closer to the backbone and increasing the bulkiness of the substituent are important to increasing the T_g. Comparisons between *n*-alkyl and alicyclic substituents indicate that, the more rigid the latter and the closer their center of mass to the backbone, the higher are the T_g values.[8] Similar trends are observed for bridged and fused ring structures where rigidity and three-dimensional size contribute to higher-than-expected T_g values. Understanding the competing effects of flexibility, rigidity, and three-dimensional size of the substituent is important for the development of new monomers and materials and their practical application.

We have demonstrated the utility of a new hybrid QSPR model that uses values of descriptors derived from a classical molecular mechanics approach based on a polymer segment to predict the glass transition temperature for acrylate and methacrylate polymers with simple ester substituents.[1,3,4] This paper extends the work to bulky, rigid substituents which are not accurately predicted by other available QSPR programs.

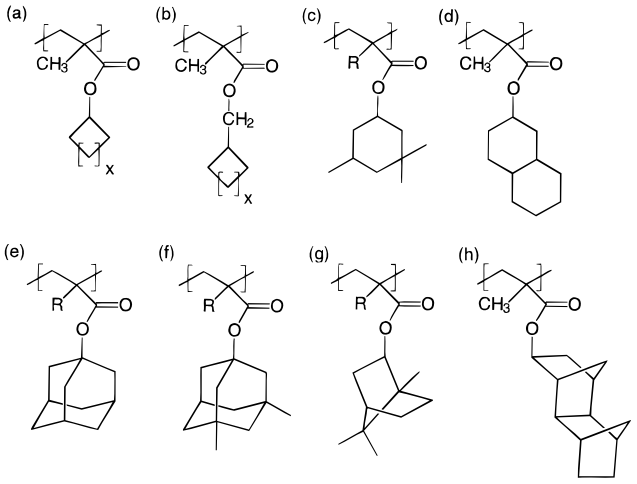

Figure 1. Partial list of acrylates and methacrylates used for this study: (a) alicyclic methacrylate, x = 4-8, 10, 12; (b) alicyclic methyl methacrylate, x = 4, 8; (c) 3,3,5-trimethylcyclohexyl acrylate and methacrylate; (d) 2-decahydronaphthyl methacrylate; (e) 1-adamantyl acrylate and methacrylate; (f) 3,5-dimethyladamantyl acrylate and methacrylate; (g) isobornyl methacrylate; (h) 3-tetracyclododecyl methacrylate.

Experimental Section

Polymer geometries and conformations were simulated with three different force fields: (1) consistent-valence force field (CVFF93),[12,13] (2) extensible systematic force field (ESFF),[14] and (3) polymer consistent force field (PCFF91).[14−20] All energy minimization and molecular dynamics calculations were performed with *Discover 95.0* molecular modeling software of Biosym/MSI.[14] Polymer building used *Polymerizer 8.0,* and visualization was performed with *InsightII 3.00*.[14]

The CVFF93 force field is a general valence force field.[12,13] Parameters are available for amino acids, water, and a variety of functional groups. This force field was chosen for initial repeat unit geometry optimization due to its ability to predict reasonable geometries for small molecules. Repeat units were minimized using the default optimization routine in *Discover* to a gradient norm value of 0.1 (kcal/mol)/Å before construction of polymer segments.

† University of Southern Mississippi, Department of Polymer Science, Southern Station, Box 10076, Hattiesburg, MS 39406.

⊗ Abstract published in *Advance ACS Abstracts,* December 15, 1996.

S0024-9297(96)01170-9 CCC: $12.00

The ESFF force field is a diagonal valence force field developed for the prediction of structures of both isolated molecules and condensed phases.[14] The valence bond, angle, torsion, and out-of-plane energies are used to describe the internal interactions, while van der Waals (vdW) and electrostatic energies represent nonbonded interactions. To account for large deviations in bond lengths and bond angles from equilibrium geometries in various systems, a Morse function for bond deformation and a truncated cosine series for angle deformation are utilized. A novel function of "dot i" products of unit vectors along the bonds 1-2, 2-3, and 3-4 are used for torsion energies such that there is no singularity when the bond angles approach 180°, simplifying the calculation of torsion energy. A new functional form for the van der Waals energy is used such that the three terms in the nonbonded energy expression take on the same form. The advantage of this expression is that nonbonded energies can be efficiently computed using more advanced techniques such as the cell multipole method and methodologies based on fast Fourier transforms.[14]

The PCFF91 force field is an extension of the CFF91 force field and is designed to account for properties of very diverse systems, i.e., isolated small molecules, condensed systems, and macromolecules.[14−20] It uses anharmonic function forms to describe bond, angle, and torsion deformations. The PCFF91 force field contains a term for the Coulombic interaction of the partial atomic charges and one for the van der Waals interaction. Within the PCFF91 force field, a number of functional groups have been explicitly parameterized on the basis of quantum mechanics calculations and molecular simulations (e.g., esters and alkanes). PCFF91 has been shown to accurately describe the conformational geometries and energies of condensed phase systems.[21]

Polymers were constructed using *Polymerizer 8.00* with a meso dyad probability value equal to 0.35 for each force field. This corresponds to the average tacticity experimentally observed for bulky substituted methacrylates. The polymers were constructed using head-to-tail addition of the minimized repeat units. The initial dihedral angles for the backbone were set to a *cis*−*trans*−*cis* conformation because this resulted in a linear starting structure and a good distribution of substituents around the polymer backbone. Twenty repeat units were used to obtain the results described here; this was previously shown to adequately reflect an average number of different conformations for each repeat unit dependent on the neighboring repeat unit geometries and interactions.[1−4]

The ESFF and PCFF91 force fields were utilized for both static and dynamic calculations of the polymer segments. For the treatment of nonbonded interactions, two different methods were employed. In the ESFF case, the cell multipole method (CMM) was used with 26 immediate neighbor cells and a distance dependent dielectric value ($\epsilon = 1r$). The CMM for nonperiodic systems provided a more rigorous and efficient treatment of nonbonded interactions than the application of typical cutoff limits.[14] For PCFF91 minimization, the atom-based cutoffs were used for the treatment of nonbonded terms with the default cutoff of 9.5 Å and a buffer width of 0.5 Å, yielding a reasonable approximation for van der Waals interaction potential.[14] The atom-based cutoff generates a list of all atoms within the cutoff distance of each atom for calculating the electrostatic and Coulombic interactions. For static minimization, the steepest descent minimization algorithm was used initially with a step of 0.3 Å when the conformations were far from the minimum. The minimization algorithm was switched to the conjugate gradient algorithm after a gradient norm convergence at 100.0 (kcal/mol)/Å. The conjugate gradient method was stopped after a gradient convergence value of 0.1 (kcal/mol)/Å. Typical CPU time for this type of minimization on 400 to 1000 atoms was from 1 min to 70 min on a wide node of the IBM 9076 SP2 at the Complexe de Calcul de Saint Jérôme, Marseille. An example of an initial conformation and the ones resulting from static and dynamic minimization routines are shown in Figure 2.

Molecular dynamic simulations were used to generate another group of polymer structures that had more randomized conformations of substituents. The ESFF and PCFF91 force fields were used; after an initial partial minimization, molecular dynamic simulations were performed. The backbone atoms were fixed in position and bond lengths were constrained for all atoms during dynamic simulations using the RATTLE algorithm (velocity version of SHAKE algorithm[22]) while the substituent groups were allowed conformational freedom. A NVT ensemble and direct velocity scaling were used during simulation at a temperature of 900 K for 1000 steps (1 fs per step). The high temperature was used to rapidly randomize the conformations of the substituents. The total simulation time of 1 ps resulted in an equilibrated total energy term at 900 K; the effect of using a longer simulation time is currently being investigated. After the MD simulations, the structures were relaxed again by unfixing the backbone and applying the same minimization routine as for static calculations. Applying molecular dynamics resulted in a distribution of substituent conformations and gives a more accurate picture of "free" space around the structures (Figure 2).

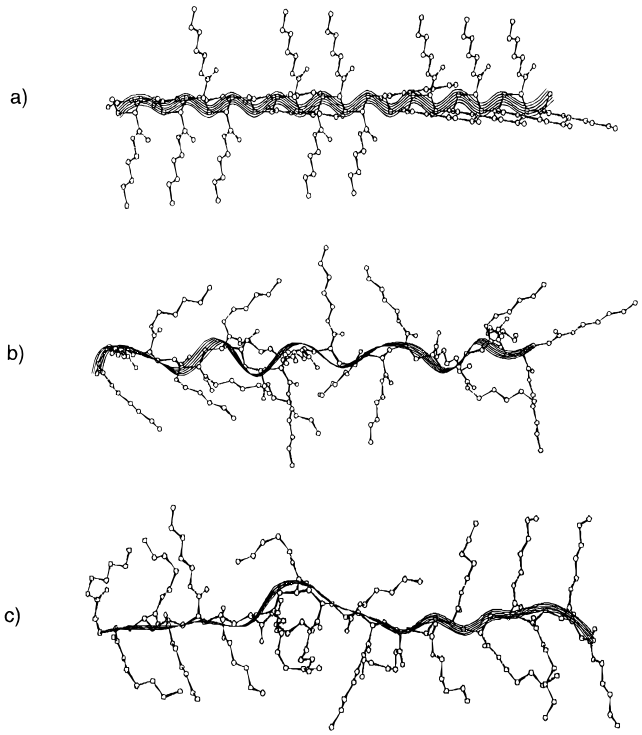

Figure 2. 2D representation of (a) the initial conformation, (b) the conformation after static minimization, and (c) the conformation after dynamic minimization. Hydrogen atoms are not shown, and the backbone atoms are highlighted by the ribbon.

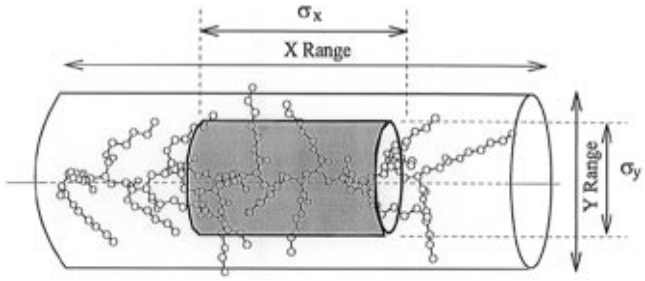

Figure 3. Example of the volume and standard deviation values used to define an elliptical volume.

The volume descriptor was calculated for each polymer segment studied. *Discover 95.0* was used to define principal axes (*x*, *y*, *z* directions) based on the position of the atoms and where each atom had an equal weight. Standard deviation values in the *x*, *y*, *z* directions were calculated and used to define an elliptical cylinder representing the space around the polymer backbone (Figure 3). This elliptical cylinder takes

Table 1. Polymer and T_g Values Used to Make the Multivariable Linear Regression Analysis To Solve for Constants *A, B,* and *C*[a]

no.	structure	exp T_g (K)	ref
1	*n*-nonyl acrylate	184	27
2	*n*-octyl acrylate	208	27
3	*n*-pentyl acrylate	216	27
4	*n*-butyl acrylate	224/219	28/23
5	*n*-propyl acrylate	228	27
6	ethyl acrylate	251	28/23
7	*n*-octyl methacrylate	253	28/23
8	*n*-hexyl methacrylate	273/268	29/27
9	*n*-pentyl methacrylate	268	27
10	methyl acrylate	282	28
11	*n*-butyl methacrylate	292/310/297	28/23/30
12	*n*-propyl methacrylate	308/319	28/29
13	ethyl methacrylate	338/343	28/30
14	methyl methacrylate	378/380/400	28/30/6
15	isobutyl acrylate	230	31
16	3,3,5-trimethylcyclohexyl acrylate	288	23
17	neopentyl acrylate	295	32
18	cyclohexyl methacrylate	356/377/384	23/31/7
19	*tert*-butyl methacrylate	380	31
20	3,3-dimethyl-2-butyl methacrylate	381	27
21	adamantyl methacrylate	532/456	6
22	*dl*-isobornyl methacrylate	396/464/443	33/7/23
23	3,5-dimethyladamantyl methacrylate	467	6

[a] The values listed first were used for the linear regression.

Table 2. List of Polymers That Were Not Included in the Multivariable Linear Regression Analysis[a]

no.	structure	exp T_g (K)	ref
24	2-methylbutyl acrylate	241	27
25	*sec*-butyl acrylate	253	31
26	*tert*-butyl acrylate	316	31
27	*n*-hexyl acrylate	216	31
28	*n*-heptyl acrylate	213	31
29	cyclohexyl acrylate	N/A	
30	1-adamantyl acrylate	426	6
31	3,5-dimethyladamantyl acrylate	378	6
32	cyclobutyl methacrylate	351	8
33	cyclopentyl methacrylate	348	8
34	cycloheptyl methacrylate	N/A	
35	cyclooctyl methacrylate	346	8
36	cyclodecyl methacrylate	331	8
37	cyclododecyl methacrylate	329	8
38	3,3,5-trimethylcyclohexyl methacrylate	398	23
39	2-decahydronaphthyl methacrylate	418	7
40	3-tetracyclododecyl methacrylate	477	7
41	cyclobutylmethyl methacrylate	N/A	
42	cyclooctylmethyl methacrylate	326	8
43	3,3-dimethylbutyl methacrylate	318	27
44	neopentyl methacrylate	299	27
45	isopropyl methacrylate	358	31
46	isobutyl methacrylate	326	31
47	*sec*-butyl methacrylate	333	31

[a] This list represents the structures where the T_g's were calculated and compared to literature reported T_g values.

into account the space occupied by the atoms and the "free" space between the atoms (termed TSSV, total space around a standard deviation volume for a polymer segment).[1,4]

Repeat units and experimental T_g values were obtained from a variety of literature sources. Tables 1 and 2 list the experimental T_g values used in this study. Caution is advised when using literature values for correlations. We have discovered some cases where reported T_g values for the same polymer differ by as much as 80 K. Deciding which values to use for the initial correlation and the predictive evaluation is not easy. We must develop a reliable database of values based on in-house synthesized, purified and characterized samples. Work on this is currently underway.

Results and Discussion

Arriving at a satisfactory QSPR equation is an iterative process. In earlier work,[1−4] we demonstrated that the T_g value of aliphatic linear and branched acrylates and methacrylates could be calculated using the following equation:

$$T_g = A + B\left(\frac{E_{vdW} \times MW}{TSSV}\right) \quad (1)$$

where A and B are constants, E_{vdW} is the intramolecular van der Waals energy, TSSV is the volume (total space around a standard deviation volume), and MW is the molecular weight of a repeat unit.[4]

To arrive at this equation, we used the definition that the T_g is a macroscopic change from a glassy material to a less ordered rubbery material that typically involves segmental motion. The increase in the movement of atoms and segments requires that the energy exist for their movement, and that there is either a place for the movement to occur (i.e. free volume) or that the segments can move in cooperation with each other (i.e. cooperative motion). This energy change is related to (1) the shape and size of the substituents directly attached to the polymer backbone, (2) the conformational mobility of the polymer chain itself, and (3) the molecular shape of the substituents located away from the backbone. The energies of these conformational changes can be evaluated with molecular mechanics techniques. The force fields used in this investigation are of the class II type and reflect atom parameters based on both gas and condensed phase structures. As a consequence, these force fields indirectly reflect a condensed phase, but not explicitly the interchain interactions or other influences such as entanglements in the polymer matrix. At the present stage, and to simplify calculations, we have not yet taken these two points into account; the assumption that they do not have a large influence on the T_g of aliphatic acrylate and methacrylates is confirmed by the excellent agreement between the calculated and measured T_g of the polymers under investigation (see Table 4 and 5). As a consequence, our model is not related to cohesive energy density. To allow reasonable calculation times, we do not consider the entire polymer matrix, but only a limited polymer segment of 20 repeat units, approximately 40 Å long. Use of this segment size not only reflects an adequate number of available molecular conformations[1,3,4] but also allows calculating T_g values which are in agreement with measured values. In our initial work,[1,3,4] we considered alkyl methacrylates because nonbonded interactions do not play an important role determining properties. This allowed us to derive an equation of type 1 with A and B coefficients specifically optimized for alkyl acrylates and methacrylates. Applying this equation with these A and B constants to polymers where the alkyl groups have been replaced by mono- or polycyclic (fused or bridged) cycloalkyl groups resulted in large errors for calculated T_g values compared to experimental ones (Figure 4). We concluded that, for these types of structures, the vdW nonbonded energy alone is not sufficient to describe the T_g.

An additional energy contribution was needed to describe the alicyclic and bridged structures. It was necessary to include an internal energy term (bond stretching, valence angle deformation, torsional angle deformation energy) to improve the linear fit to experi-

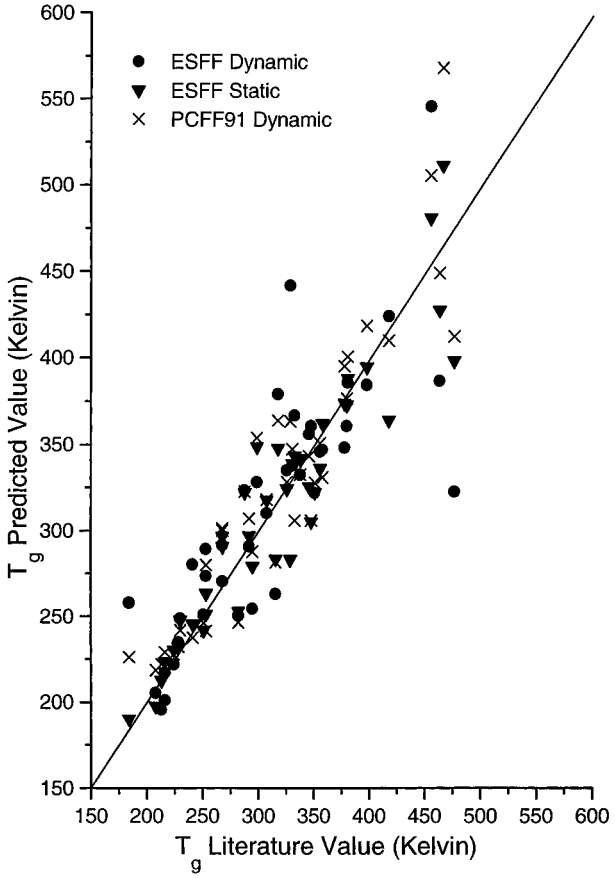

Figure 4. Example of the calculated T_g values using the fit parameters from ref 4. The solid line represents a perfect prediction.

Table 3. Statistical Results for all the Acrylates and Methacrylates Included in Table 1 for Multivariable Linear Regression

minimization technique	$A(\sigma)^a$	$B(\sigma)^a$	$C(\sigma)^a$	r^2	σ (K)
ESFF static	215.57(6.7)	−0.46(0.16)	3.56(0.24)	0.96	17.4
ESFF dynamic	208.5(7.4)	−0.30(0.18)	3.45(0.27)	0.96	19.0
PCFF91 dynamic	212.0(9.00)	0.21(0.11)	3.04(0.22)	0.91	27.2

[a] σ = standard deviation.

mental T_g values for all the structures included in this study. The original QSPR[1,4] (eq 1) was therefore modified to the following form:

$$T_g = A + B\left(\frac{E_{int} \times MW}{TSSV}\right) + C\left(\frac{E_{vdW} \times MW}{TSSV}\right) \quad (2)$$

where A, B, and C are fit parameters, E_{vdW} is the intramolecular van der Waals energy, E_{int} is the internal energy, TSSV is the volume, and MW is the molecular weight of a repeat unit.

Using the structures in Table 1, multiple-variable linear regression was used to solve for the constants A, B, and C. The structures in Table 1 were chosen because they yielded a large experimental T_g range that would not bias the results toward low or high T_g materials. Two force fields and three minimization techniques were investigated. In most cases, structures were easily minimized, except in the case of poly(cyclooctylmethyl methacrylate) where ring overlapping or catenation occurred on minimization.

Table 3 lists the statistical results obtained with each minimization technique. The fit parameters A, B, and C are very similar (within a standard deviation of each other). This indicates that each force field and minimization technique results in similar calculated T_g values, especially if the standard error on the measured T_g's is taken into consideration. It should be noted that the energy and volume values are different for each force field; this results from each having different sets of atomic parameters and potential types. A single equation was derived that does not depend on the force field nature, but rather on the molecular features of the monomer and repeat unit segments used in the calculation.

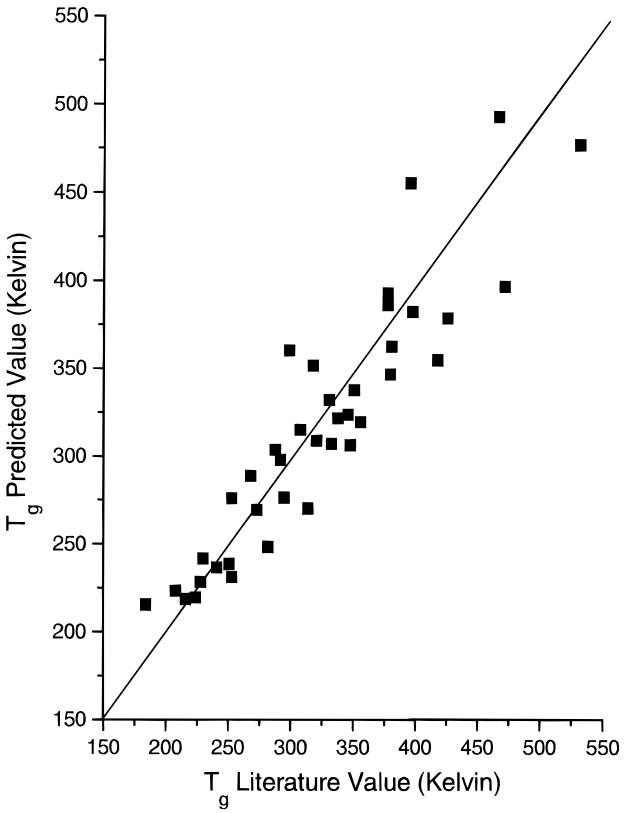

Figure 5. Glass transition temperature predictions using the PCFF91 dynamic minimization technique. The solid line represents a perfect prediction.

Figure 5 illustrates the usefulness of the constants derived from eq 2 for predictive purposes. Calculated values are listed in Table 4 for selected molecules. The standard error for the 16 structures in Table 4 is 13.4%, 11.6%, and 8.4%, with respect to each force field. This is in the range of errors that can be expected from the experimental T_g's found in the literature, i.e., errors due to different sample preparation methods and T_g measurement techniques.

Another comparison that can be made is to other QSPR models.[23−26] Both Hopfinger's and Bicerano's QSPR models are based on the premise that individual group contributions are not required because they can be calculated. The first comparison made used the experimental acrylate and methacrylate T_g values reported by Hopfinger, Koehler and Pearlstein,[23] where the T_g values were all obtained using the same technique; this should give the best correlation because it eliminates sampling variables. After multiple-variable linear regression analysis on this data set, we obtained an r^2 value of 0.90 and a standard deviation of 20 K using the EVM model, compared to r^2 of 0.91 and standard deviation of 19 K obtained by Hopfinger, Koehler, and Pearlstein (Table 5).[23] A more recent

Table 4. Predicted T_g Values Using Constant Values Listed in Table 3[a]

structure	exp T_g (K)	ESFF static	ESFF dynamic	PCFF91 dynamic	Bicerano[b]
cyclobutyl methacrylate	351	246	268	338	367
cyclopentyl methacrylate	348	278	287	306	370
cyclohexyl methacrylate	356	332	335	319	371
cyclooctyl methacrylate	346	305	306	324	373
cyclodecyl methacrylate	331	290	306	332	376
cyclobutylmethyl methacrylate		228	247	323	339
cyclooctylmethyl methacrylate	326	N/A	301	N/A	344
3,3,5-trimethylcyclohexyl acrylate	288	297	300	304	358
3,3,5-trimethylcyclohexyl methacrylate	398	380	360	382	391
2-decahydronaphthyl methacrylate	418	338	340	355	376
1-adamantyl acrylate	426	387	412	378	355
1-adamantyl methacrylate	532	510	500	477	390
3,5-dimethyladamantyl acrylate	378	427	425	386	391
3,5-dimethyladamantyl methacrylate	467	508	521	493	421
isobornyl methacrylate	396	392	397	455	400
3-tetracyclododecyl methacrylate	477	270	312	398	N/A

[a] The absolute error is 13.4%, 11.6%, 8.4%, and 9.7% with respect to each method. [b] Bicerano values were obtained from a "designer correlation" using *Synthia* and based on the molecules in Table 1.[14]

Table 5. Comparison between the Experimental and Calculated T_g Values with the EVM PCFF91 Model, the Hopfinger Model, and the Bicerano Model[a]

structure	exp T_g[23] (K)	EVM	Hopfinger	Bicerano
methyl acrylate	282	266	273	266
ethyl acrylate	251	239	226	281
n-butyl acrylate	219	220	209	249
isobutyl acrylate	230	242	259	290
sec-butyl acrylate	253	231	246	295
tert-butyl acrylate	314	270	300	351
methyl methacrylate	378	393	359	327
ethyl methacrylate	338	322	288	330
isopropyl methacrylate	354	344	344	359
n-butyl methacrylate	293	298	262	289
isobutyl methacrylate	321	309	337	329
sec-butyl methacrylate	333	307	318	333
tert-butyl methacrylate	380	347	402	385
n-hexyl methacrylate	268	269	254	246
n-octyl methacrylate	253	276	250	203
isobornyl methacrylate	443	455	418	383

[a] Predictions were made using T_g experimental values obtained from Hopfinger, Koehler, and Pearlstein[23] and deriving new fit parameters for the EVM model and a "designer correlation" for the Bicerano model.

universal QSPR equation has been derived by Hopfinger, Koehler, and Pearlstein[23,24] which is based on a broader set of polymer structures. Comparisons of our QSPR equation to any universal equation (such as theirs) at this time is not reasonable because we have not developed the additional parameters needed for other types of structures and interactions.

Another comparison was made with Bicerano's model,[26] which is also a universal model derived from a large number of different polymers. We have used Bicerano's approach and descriptors to calculate a "designer correlation" based on molecules listed in Table 5. Values of r^2 (0.69) and σ (36 K) were considerably worse than both ours and Hopfinger's. We also made a "designer correlation" using the 23 molecules in Table 1 to compare directly with the EVM-calculated T_g values in Table 4 ($r^2 = 0.73$ and $\sigma = 47$ K compared to our values of 0.91 and 27 K). The absolute standard error for this set using the same molecules is 9.7% compared to 8.4% for the PCFF91 force field. Bicerano's predicted values are quite good for these structures except for the adamantyl-substituted structures; this was one of the main concerns that led to our development of a new QSPR model (Figure 6).

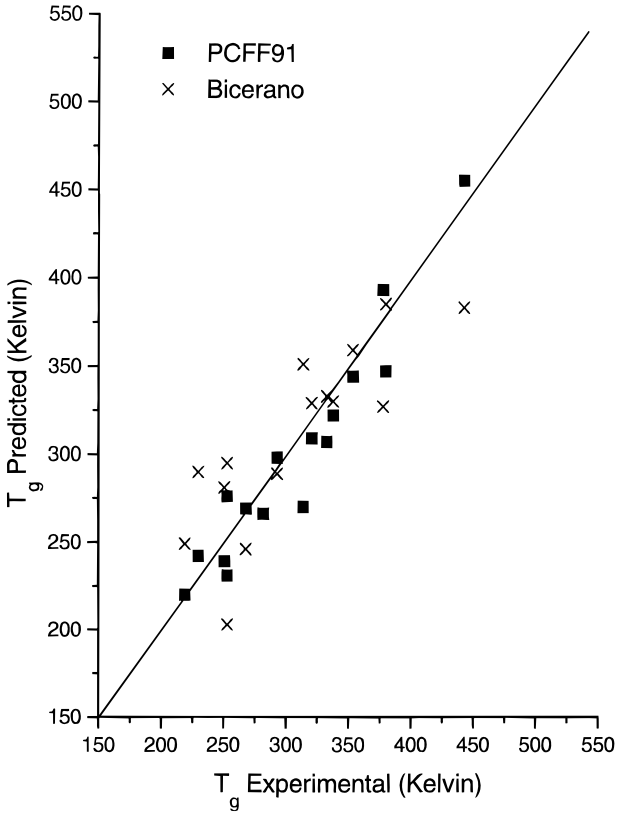

Figure 6. Comparison between predicted T_g values for the PCFF91 EVM method and a "designed correlation" using Bicerano's method (*Synthia*) for molecules listed in Table 5. The solid line represents a perfect prediction.

Conclusions

The EVM QSPR approach is still limited (as are all QSPR methods) by the validity of the experimental data used to derive the coefficients of the QSPR correlation. In particular, literature values reported for T_g's are very sensitive to sample history and experimental conditions; e.g., widely different T_g values can be found for the same structure. To overcome this problem, development of a database of T_g values measured in a consistent manner on purified samples is being carried out to improve future QSPR correlations. It appears that the accuracy of calculated values depends both on the accuracy of the database values used to evaluate correlation parameters and on the model and methods used to evaluate the

correlation parameters. The EVM model is as good as previous models in terms of accuracy of calculated T_g values of "typical" polymers, and better for novel bulky substituents; i.e., based on the small range of bulky substituents used, a standard deviation of ~20 K was obtained. Calculating T_g values for novel structures is simple and requires only that a polymer segment be described in terms of its energy and volume, as determined by molecular mechanics calculations; it does not require a previously known group contribution value. The EVM equation accounts for flexibility, rigidity, and three-dimensional size of substituents for the series of aliphatic acrylates and methacrylates presented here. The apparent indifference of the results to the choice of force fields may be an artifact of the restricted families of polymers examined. It should become more significant when attempting to develop a more general QSPR correlation; this will require continued investigations including incorporation of Coulombic and electrostatic descriptors (as was pointed out by a referee). At this point of our model development, we have only used the EVM approach to calculate T_g values. Additional computational tools are required to calculate other properties of polymers. We hope to extend this model to other acrylate and methacrylate derivatives, and other families of polymers to arrive at a broad-based general purpose QSPR equation.

Acknowledgment. We thank Dr. M. Audenaert (CERDATO/ELF-ATOCHEM) for discussions on this project. We also thank Dr. Jablon (ELF-AQUITAINE) for his interest in this work and for financial support (stipend to C.C.C.), as well as the Council of Provence Alpes Cote d'Azur and the ANVAR (scholarships to P.C.). We are grateful to the "Complexe de Calcul de Marseille St. Jérôme, France", for computation time on an IBM 9076 SP2, as well as to IBM France for technical support.

References and Notes

(1) Camelio, P.; Lazzeri, V.; Waegell, B. *Polym. Prepr.* (*Am. Chem. Soc., Div. Polym. Chem.*) **1995**, *36* (1), 661.
(2) Ferret, N. Thèse de Doctorat en Sciences, Universite d'Aix-Marseille III, 1992.
(3) Camelio, P. DEA, Universite d'Aix-Marseille III, 1994.
(4) Camelio, P.; Cypcar, C. C.; Lazzeri, V.; Waegell, B. Submitted for publication.
(5) Matsumoto, A.; Tanaka, S.; Otsu, T. *Colloid Polym. Sci.* **1992**, *270*, 17.
(6) Matsumoto, A.; Tanaka, S.; Otsu, T. *Macromolecules* **1991**, *24*, 4017.
(7) Matsumoto, A.; Mizuta, K.; Otsu, T. *J. Polym. Sci.* **1993**, *31*, 2531.
(8) Mayes, J. W.; Siakali-Kioulafa, E.; Hadjichristidis, N. *Macromolecules* **1990**, *23*, 3530.
(9) Pateropoulou, D.; Siakali-Kioulafa, E.; Hadjichristidis, N.; Nan, S.; Mays, J. W. *Macromol. Chem. Phys.* **1994**, *195*, 173.
(10) Mathias, L. J.; Jensen, J. L.; Reichert, V. T.; Lewis, C. L.; Tullos, G. L. In *Step-Growth Polymers for High-Performance Materials: New Synthetic Methods*; ACS Symposium Series No. 624; Hedrick, J. L., Labadie, J. W., Eds.; American Chemical Society: Washington, DC, 1996.
(11) Tsuda, T.; Mathias, L. J. *Polymer* **1994**, *35*, 3317.
(12) Bauber-Osguthorpe, P.; Roberts, V. A. *Struct., Funct., Genet.* **1988**, *4*, 31.
(13) Hagler, A. T.; Lifson, V.; Dauber, P. *J. Am. Chem. Soc.* **1979**, *101*, 5122.
(14) Biosym/MSI, San Diego. *Discover 3.0/95.0 User Guide*, October 1995.
(15) Maple, J. A.; Hwang, M. J.; Stockfisch, T. P.; Dinur, U.; Waldman, M.; Ewig, C. S.; Hagler, A. T. *J. Comput. Chem.* **1994**, *15*, 162.
(16) Hwang, M. J.; Stockfisch, T. P.; Hagler, A. T. *J. Am. Chem. Soc.* **1994**, *116*, 2512.
(17) Sun, H.; Mumby, J. R.; Maple, J. R.; Hagler, A. T. *J. Am. Chem. Soc.* **1994**, *116*, 2978.
(18) Sun, H. *J. Comput. Chem.* **1994**, *15*, 7.
(19) Sun, H. *Macromolecules* **1995**, *28*, 701.
(20) Hill, J. R.; Sauer, J. *J. Phys. Chem.* **1994**, *98*, 1238.
(21) Trommsdorff, U.; Tomka, I. *Macromolecules* **1995**, *28*, 6128.
(22) Ryckaert, J. P.; Ciccotti, G.; Berendson, H. J. C. *J. Comput. Phys.* **1977**, *23*, 327.
(23) Hopfinger, A. J.; Koehler, M. G.; Pearlstein, R. A. *J. Polym. Sci., Part B: Polym. Phys.* **1988**, *26*, 2007.
(24) Koehler, M. G.; Hopfinger, A. J. *Polymer* **1989**, *30*, 116.
(25) Hopfinger, A. J.; Koehler, M. G. In *Computer Simulation of Polymers;* Colbourn, E. A., Ed.; Longman Scientific and Technical: Essex, England, 1994.
(26) Bicerano, J. *Prediction of Polymer Properties*; Marcel Dekker Inc.: New York, 1993.
(27) Brandrup, J.; Immergut, E. H. *Polymer Handbook*, 3rd ed.; John Wiley & Sons: New York, 1990.
(28) Seitz, J. T. *J. Appl. Polym. Sci.* **1993**, *49*, 1331.
(29) Garwe, F.; Schonhals, A.; Lockwenz, H.; Beiner, W.; Shroter, K.; Donth, E. *Macromolecules* **1996**, *29*, 247.
(30) Ribelles Gomez, J. L.; Monleon Pradas, M.; Vidaurre Garayo, A.; Romero Colomer, F.; Mas Estelles, J.; Duenas Mesegner, J. M. *Macromolecules* **1995**, *28*, 3878.
(31) Mark, H. F.; Bikales, N. M.; Overberger, C. G. *Encyclopedia of Polymer Science and Engineering*, 2nd ed.; John Wiley & Sons: New York, 1990.
(32) Krause, S.; Gornmley, J. J.; Roman, N.; Shetter, J. A.; Watanabe, W. H. *J. Polym. Sci., Part A* **1965**, *3*, 3573.
(33) Alvarez, F.; Colmenero, J.; Wang, C. H.; Xia, J. L.; Fytas, G. *Macromolecules* **1995**, *28*, 6488.

MA961170S